

# High-Temperature Synthesis and Structures of Perovskite and $n = 1$ Ruddlesden–Popper Tantalum Oxynitrides

Simon J. Clarke,\*† Katharine A. Hardstone,† Charles W. Michie,‡ and Matthew J. Rosseinsky\*,‡

*Inorganic Chemistry Laboratory, Department of Chemistry, University of Oxford, South Parks Road, Oxford OX1 3QR, U.K., and Department of Chemistry, University of Liverpool, Liverpool L69 7ZD, U.K.*

Received December 27, 2001. Revised Manuscript Received April 8, 2002

The perovskite- and  $K_2NiF_4$ -structure group 5 oxynitrides  $SrTaO_2N$ ,  $BaTaO_2N$ ,  $Sr_2TaO_3N$ , and  $Ba_2TaO_3N$ , previously prepared by reacting oxide precursors with ammonia, may also be prepared by the reaction between the appropriate alkaline earth oxide and  $TaON$  at 1500 °C under 1 atm of pure nitrogen gas for a few hours. The nitrogen atmosphere is essential to prevent reduction of  $Ta^V$ , and the method of inductive heating ensures that the nitrogen atmosphere above the sample is maintained free of oxygen or water.  $SrTaO_2N$  crystallizes in  $I4/mcm$  with  $a = 5.694\ 11(7)$  Å,  $b = 8.0658(2)$  Å, and  $Z = 4$ . The oxide and nitride anions are almost completely disordered, as observed when the material is made by nitridation of a pure oxide precursor using ammonia at 900–1000 °C, but contrasting with the full O/N order observed when such nitridation is mineralizer assisted. The detailed structure of  $Ba_2TaO_3N$  is reported for the first time: this compound adopts the  $K_2NiF_4$  type structure with full O/N order in space group  $I4/mmm$  with  $a = 4.115\ 08(3)$  Å,  $c = 13.3778(1)$  Å, and  $Z = 2$  and is isostructural with the strontium analogue ( $Sr_2TaO_3N$ :  $I4/mmm$ ,  $a = 4.038\ 99(4)$  Å,  $c = 12.6007(3)$  Å, and  $Z = 2$ ). O/N disorder is favored in perovskite-structure oxynitrides, but in layered  $K_2NiF_4$ -structure materials O/N ordering is the norm, with the ordering scheme dictated by the competition between cations of differing electronegativity for the anions.

## Introduction

Ternary transition metal oxynitrides are a growing class of material. The continuous substitution of oxide by nitride is an attractive way of modifying the structures and electronic properties of materials in a continuous way, and the possibility of crystallographic ordering between the oxide and nitride anions offers the prospect of realizing polar noncentrosymmetric materials<sup>1</sup> or materials with layered characteristics. Jansen and co-workers<sup>2</sup> have recently demonstrated that the perovskites  $Ca_xLa_{1-x}TaO_{1+x}N_{2-x}$ , representing the solid solution between  $CaTaO_2N$  and  $LaTaON_2$ , have a range of yellow to red colors and are possible pigments to replace cadmium-containing materials.

A majority of oxynitrides have been synthesized by the reaction between a metal oxide and flowing ammonia gas at temperatures up to 1000 °C. The degree of substitution of nitride for oxide in the products depends on the electropositivity and oxophilicity of the metals present. The nitridation of a  $SrTaO_{3.5}$  precursor produces a limiting composition of  $SrTaO_2N$ .<sup>3–5</sup>

We are exploring the use of high-temperature con-proportionation of binary oxides, nitrides, and oxynitrides under pure nitrogen gas in a radio frequency induction furnace in an attempt to limit the oxide content of the products. This route has previously yielded many new nitrides, notably in the groups of DiSalvo and co-workers<sup>6</sup> and Schnick and co-workers.<sup>7</sup> Inductive heating of a metal crucible containing the sample enables an atmosphere of pure nitrogen to be maintained over the sample even at 1500 °C or above. Here we report that several ternary tantalum (V) oxynitrides may be synthesized by this route and compare them with the corresponding compounds synthesized by nitridation with ammonia. The structure of  $Ba_2TaO_3N$  is reported for the first time. Our high-temperature synthetic method also allows us to approach the thermodynamic limit with regard to crystallographic O/N order/disorder. Our results support the conclusion that O/N disorder is thermodynamically favored in the perovskite-structure materials at high temperatures but that O/N order is favored in the lower dimensionality  $K_2NiF_4$ -structure materials.

\* To whom correspondence should be addressed.

† University of Oxford.

‡ University of Liverpool.

(1) Marchand, R.; Pastuszak, R.; Laurent, Y.; Roult, G. *Rev. Chim. Miner.* **1982**, *19*, 684.

(2) Jansen, M.; Letschert, H. P. *Nature* **2000**, *404*, 980.

(3) Günther, E.; Hagenmayer, R.; Jansen, M. Z. *Anorg. Allg. Chem.* **2000**, *626*, 1519.

(4) Pors, F.; Bacher, P.; Marchand, R.; Laurent, Y.; Roult, G. *Rev. Int. Hautes Temp. Refract.* **1987**, *24*, 239.

(5) Marchand, R.; Pors, F.; Laurent, Y. *Rev. Int. Hautes Temp. Refract.* **1986**, *23*, 11.

(6) Balbarin, V.; Van Dover, R. B.; DiSalvo, F. J. *J. Phys. Chem. Solids* **1996**, *57*, 1919.

(7) Schnick, W.; Huppertz, H.; Lauterbach, R. *J. Mater. Chem.* **1999**, *9*, 289.

**Table 1. Summary of Syntheses of Perovskite- and  $K_2NiF_4$ -Structure Oxynitrides**

reactants	T/°C	conditions <sup>a</sup>	duration/h	color	identified products
CaO + TaON	1200	$N_2$ 1 atm	2 + 2 + 2 + 2	dark green	$CaTaO_2N$ , $Ta_4N_5$
CaO + TaON	1400	$N_2$ 1 atm	1	green	$CaTaO_2N$ , $TaN$
SrO + TaON	1350	Ni tube	60	green	$SrTaO_2N$ , $SrO$ , $TaN$
SrO + TaON	1500	$N_2$ 1 atm	3	brown	$SrTaO_2N^b$
BaO + TaON	1200	vacuum	1	brown	$BaTaO_2N$ , $TaN$
BaO + TaON	1600	vacuum	1	brown	$BaTaO_2N$ , $Ta_2N$
BaO + TaON	1500	$N_2$ 1 atm	3	brown	$BaTaO_2N$
2CaO + TaON	1500	$N_2$ 1 atm	3	green	$CaTaO_2N$ , $CaO$ , $TaN$
2SrO + TaON	1350	Ni tube	60	orange	$Sr_2TaO_3N$ , $SrTaO_2N$ , $TaN$
2SrO + TaON	1500	$N_2$ 1 atm	3	orange	$Sr_2TaO_2N^b$
2BaO + TaON	1500	$N_2$ 1 atm	3	orange/brown	$Ba_2TaO_3N^b$

<sup>a</sup> The conditions used were as follows: inductive heating under 1 atm of clean  $N_2$ , inductive heating under a static vacuum of  $10^{-2}$  mbar, or reaction in a nickel tube sealed under 1 atm of clean Ar. <sup>b</sup> Samples used for neutron diffraction investigations.

## Experimental Section

TaON was prepared by reacting  $Ta_2O_5$  (ALFA AESAR 99.993%) with flowing ammonia gas (BOC 99.98%) at 850 °C in a flow apparatus, described previously.<sup>8</sup> The ammonia was flowed through a saturated solution of ammonia in water before entering the reaction vessel, and was flowed at the rate 100  $cm^3$  min<sup>-1</sup> over the sample for 15 h. The use of moist ammonia to make TaON<sup>9</sup> prevents the formation of  $Ta_3N_5$ . Combustion analysis for nitrogen and thermogravimetric oxidation of our TaON sample indicated compositions of  $TaO_{0.95(3)}N_{1.03(3)}$  and  $TaO_{1.03(3)}N_{0.98(3)}$ , respectively. The alkaline earth oxides were prepared by decomposition of the carbonates contained in an alumina tube under vacuum:<sup>10</sup>  $SrCO_3$  (ALFA AESAR 99.994%) was decomposed overnight at 850 °C under  $2 \times 10^{-2}$  mbar with the temperature then raised to 1100 °C for a final 3 h of firing;  $BaCO_3$  (ALFA AESAR 99.95%) was decomposed overnight at 950 °C under  $2 \times 10^{-2}$  mbar with a final firing at 1100 °C. The phase purity of the products was confirmed using powder X-ray diffraction (PXRD), combustion analysis for nitrogen, and thermogravimetric analysis (TGA) during oxidation.

In the preparation of the ternaries, all the manipulations were carried out in a Glovebox Technology drybox with a constantly recirculated argon atmosphere with an  $O_2$  and  $H_2O$  content of less than 5 ppm. Several of the reagents and products are air sensitive, and our synthetic method requires that the reagents are free of adsorbed moisture, which would be a source of unwanted additional oxygen in the system. Light yellow-green TaON was ground with the appropriate stoichiometric amount of white alkaline earth oxide to give a total mass of 1–2 g and pressed into a pellet at the pressure 4 kbar. The pellets were heated either in an induction furnace (at up to 1600 °C) or in sealed nickel tubes (at up to 1350 °C), as summarized in Table 1. For reactions carried out using inductive heating, the pellet was loaded into a molybdenum crucible (12.5 mm diameter and 50 mm long), which was suspended using a molybdenum wire inside a silica tube with an internal diameter of 22 mm, equipped with a valve at one end. The tube was evacuated of drybox argon to  $10^{-2}$  mbar and filled with 1 atm of nitrogen gas (BOC 99.999%;  $O_2$  2 ppm,  $H_2O$  3 ppm) which had been purified by passing over titanium wire held at 800 °C. The tube was constructed in a similar way to that in ref 6 such that the purified  $N_2$  gas was allowed to flow over the opening of the tube and thus 1 atm of  $N_2$  was maintained over the sample. The tube was placed vertically inside the 5 cm diameter and 12 cm long coil of a Stanelco 15 kW high-frequency induction furnace. The molybdenum crucible, and therefore also the sample, was heated inductively, and the temperature was measured using a Raytek two-color infrared pyrometer. A coil of zirconium foil placed at the mouth of the molybdenum crucible acted as an additional oxygen/

water scavenger. Under these conditions, the silica tube reaches a temperature of only about 100 °C even when the crucible is at 1500 °C, and this eliminates a potential source of oxygen or water in the system. After heating, the furnace power was turned off and the sample cooled below 600 °C in less than 1 min. Some reactions were carried out in a similar way except that the reaction vessel was not filled with  $N_2$  and the crucible and sample were instead heated under a static vacuum of  $10^{-2}$  mbar. Reactions in sealed nickel tubes were carried out by sealing the pellets in nickel tubes (purity 99.99%; 9 mm diameter; 0.5 mm wall thickness) using an arc furnace under 1 atm of argon purified by flowing over Ti wire held at 800 °C. The tubes were heated in a tubular resistance furnace under a protective blanket of flowing argon gas. Phase pure target materials were only obtained in the reactions under  $N_2$  using the induction furnace and were attainable after only one treatment of a few hours at 1500 °C (Table 1). We were able to synthesize  $ATaO_2N$  and  $A_2TaO_3N$  ( $A = Sr$ ,  $Ba$ ) phase pure (according to PXRD) by this method, but we were unable to synthesize  $CaTaO_2N$  and  $Ca_2TaO_3N$  completely free of the reduced tantalum nitride phases  $TaN$  and  $Ta_5N_4$  which were identified by PXRD. This is likely a consequence of partial reduction of TaON at high temperatures competing successfully against the reaction to form the ternary phases when the least reactive of the three oxides  $CaO$ ,  $SrO$ , and  $BaO$  is used. Reduced tantalum nitrides were also invariably produced in the reactions carried out under vacuum. Reactions in sealed nickel tubes were slow at temperatures below the softening point of Ni (mp = 1453 °C) as a result of slow ionic diffusion, and these also contained reduced products; a slight bulging of the sealed tube indicated that some  $N_2$  was evolved in these reactions.

**Diffraction Measurements.** Laboratory powder X-ray diffraction to assess phase purity and determine lattice parameters was carried out using a Philips PW1050 diffractometer operating in Bragg–Brentano geometry with  $Cu K\alpha$  radiation or, for air-sensitive samples, a Siemens D5000 diffractometer operating in Debye–Scherrer geometry with  $Cu K\alpha_1$  radiation selected by a  $Ge(111)$  monochromator and with the sample ground with amorphous boron in a 1:2 sample/boron mass ratio to reduce sample absorption, and contained in a 1 mm diameter glass capillary. Neutron powder diffraction data were collected on  $SrTaO_2N$ ,  $Sr_2TaO_3N$ , and  $Ba_2TaO_3N$  using the diffractometer POLARIS at the ISIS spallation source, Rutherford Appleton Laboratory, U.K. Samples were contained in 6 mm diameter cylindrical vanadium cans.  $Ba_2TaO_3N$  hydrolyses rapidly in air, and so the can was sealed in the drybox using an indium gasket. Data were collected using detector banks located at  $2\theta$  angles of 35° ( $^3He$  tube detector), 90° ( $ZnS$  scintillator), and 145° ( $^3He$  tube detector, highest resolution bank:  $\Delta d/d = 5 \times 10^{-3}$ ) in the  $d$ -spacing range 0.5–8 Å for a total integrated proton current at the production target of 204, 321, and 368  $\mu$ Ah for 1.7 g of  $SrTaO_2N$ , 1.6 g of  $Sr_2TaO_3N$ , and 1.5 g of  $Ba_2TaO_3N$ , respectively. X-ray and neutron powder diffraction data were analyzed using the Rietveld profile refinement suite GSAS.<sup>11</sup> Refinement against neutron data was carried out using all three detector banks simultaneously.

(8) Clarke, S. J.; Michie, C. W.; Rosseinsky, M. J. *J. Solid State Chem.* **1999**, *146*, 399.

(9) Brauer, G.; Weidlein, J.; Strähle, J. *Z. Anorg. Allg. Chem.* **1966**, *348*, 298.

(10) Brauer, G. *Handbook of Preparative Inorganic Chemistry*; Academic Press: New York, 1965.

**Table 2. Refinement Results for SrTaO<sub>2</sub>N, Sr<sub>2</sub>TaO<sub>3</sub>N, and Ba<sub>2</sub>TaO<sub>3</sub>N<sup>a</sup>**

formula	SrTaO <sub>2</sub> N	Sr <sub>2</sub> TaO <sub>3</sub> N	Ba <sub>2</sub> TaO <sub>3</sub> N
radiation	Neutron	Neutron	Neutron
instrument	POLARIS	POLARIS	POLARIS
temperature/K	298	298	298
structure type	perovskite	K <sub>2</sub> NiF <sub>4</sub>	K <sub>2</sub> NiF <sub>4</sub>
space group	<i>I</i> 4/ <i>mcm</i>	<i>I</i> 4/ <i>mmm</i>	<i>I</i> 4/ <i>mmm</i>
formula weight	314.6	418.2	467.9
<i>a</i> /Å	5.69411(7)	4.03899(4)	4.11508(3)
<i>c</i> /Å	8.0658(2)	12.6007(3)	13.3778(1)
volume/Å <sup>3</sup>	261.516(7)	205.560(8)	226.537(5)
<i>Z</i>	4	2	2
$\rho_{\text{calc}}/\text{kg}\cdot\text{m}^{-3}$	7.990(1)	6.760(2)	7.590(1)
no. of observations	13022	13376	12985
no. of variables	49	53	51
$\chi^2$ <sup>b</sup>	1.928	1.659	1.347
$WR_p$ <sup>b</sup>	0.0358	0.0269	0.0246
$R_p$ <sup>b</sup>	0.0535	0.0513	0.0470
$R(F^2)$ <sup>b</sup>	0.0575	0.0376	0.0469

<sup>a</sup> All refinements were carried out against data from three detector banks at  $2\theta = 145^\circ$ ,  $90^\circ$ , and  $35^\circ$ . <sup>b</sup> *R* factors and  $\chi^2$  refer to the refinements against all three detector banks.

## Results

**Anion Order vs Disorder in SrTaO<sub>2</sub>N.** SrTaO<sub>2</sub>N has a tetragonally distorted perovskite-related structure and has been investigated by Marchand and co-workers,<sup>4,5</sup> who reacted Sr<sub>2</sub>Ta<sub>2</sub>O<sub>7</sub> with ammonia at around 1000 °C. Their refinement of neutron powder diffraction data<sup>4</sup> in the space group *I*42*m* established that the oxide and nitride ions were close to statistically distributed over the two available anion sites. A material of this stoichiometry has recently been prepared by Jansen and co-workers<sup>3</sup> by ammonolysis at 900 °C, but with the addition of sodium chloride as a mineralizer to promote crystallization. In that case, neutron diffraction investigations revealed complete O/N order on the anion sublattice in space group *I*4/*mcm*. For our material prepared at a much higher temperature than those of the other two groups, we used the tetragonal model of ref 3 in *I*4/*mcm* as a starting model and refined it against our neutron diffraction data. The refinement results are presented in Table 2, and the fit is shown in Figure 1. In Tables 3 and 4 the structure is compared with those of the two materials synthesized by ammonolysis. Model-independent LeBail type fits to the data were unable to definitively distinguish between the two space groups *I*42*m* and *I*4/*mcm* previously used for SrTaO<sub>2</sub>N.<sup>3,4</sup> However, Rietveld refinements in the non-centrosymmetric space group *I*42*m* were unstable with respect to the anion positional and displacement parameters, and the correct space group is clearly *I*4/*mcm*. Our refinement of the anion occupancies on the two available sites, with no constraint on the overall composition but with the constraint that the two sites were fully occupied, produced the composition SrTaO<sub>2.00(3)</sub>N<sub>1.00(3)</sub>, consistent with the composition SrTaO<sub>2.01(2)</sub>N<sub>0.99(2)</sub> obtained by TGA, and clearly indicates that the higher temperature route reproduces the almost statistical O/N disorder in the material of Marchand and co-workers.<sup>4</sup> Our data allowed us to refine all atoms except Ta anisotropically, and both anion sites have similarly sized displacement ellipsoids,

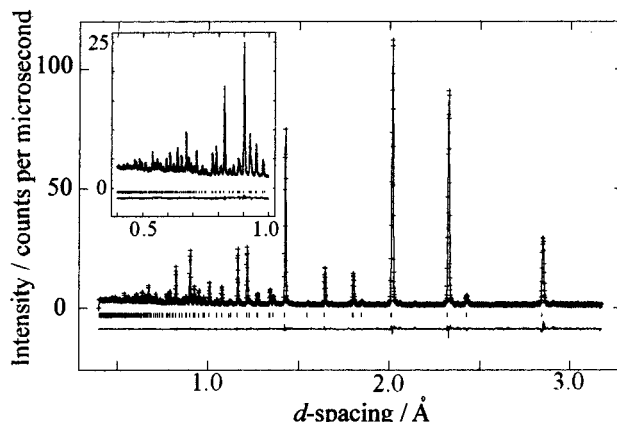


**Figure 1.** Results of the refinement of the structure of SrTaO<sub>2</sub>N against powder neutron diffraction data (145° detector bank). The measured (points), calculated (line), and difference (lower line) profiles are shown. Tick marks indicate allowed reflections.

**Table 3. Atomic Parameters for SrTaO<sub>2</sub>N from Refinement in *I*4/*mcm* against Neutron Diffraction Data**

atom	site	<i>x</i>	<i>y</i>	<i>z</i>	$100U_{\text{iso eq}}/\text{\AA}^2$	oxide fraction
Sr	4 <i>b</i>	0		0.5	0.50(1)	
Ta	4 <i>c</i>	0.5		0.5	0.74(3)	
O/N(1)	4 <i>a</i>	0		0	1.67(2)	0.54(2)
O/N(2)	8 <i>h</i>	0.768 04(9)	<i>x</i> + 0.5	0	1.32(3)	0.73(1)

<sup>a</sup> Equivalent isotropic displacement parameters are given; the anisotropic displacement parameters are shown as ellipsoids in Figure 2.

**Table 4. Selected Bond Distances (Å) for Samples of SrTaO<sub>2</sub>N Prepared at 900 °C by Ammonolysis or at 1500 °C<sup>a</sup>**

bond	bond distance/Å for disordered anions		bond distance/Å for ordered anions
	this work	ref 4	
Ta—O/N(1) [2] <sup>b</sup>	2.016 45(4)	2.022(2)	2.012
Ta—O/N(2) [4] <sup>b</sup>	2.018 41(6)	2.021(2)	2.025
Sr—O/N(2) [4] <sup>b</sup>	2.748 6(5)	2.808(3)	2.726
Sr—O/N(2) [4] <sup>b</sup>	2.847 05(4)	2.846(1)	2.852
Sr—O/N(2) [4] <sup>b</sup>	2.953 8(5)	2.909(3)	2.978

<sup>a</sup> All O/N—Ta—O/N angles are 90° or 180°. <sup>b</sup> The numbers in square brackets indicate the number of bonds or angles of a particular type.

as shown in Figure 2. Selected bond lengths and angles are given in Table 4, where the two polymorphs of SrTaO<sub>2</sub>N are compared.

In the material produced by Jansen and co-workers,<sup>3</sup> there is complete O/N ordering, and the framework of TaO<sub>4</sub>N<sub>2</sub> octahedra is composed of linear N—Ta—N chains extending along the tetragonal axis and corner-linked TaO<sub>4</sub> squares in the *ab* plane which are rotated with respect to each other about the tetragonal axis parallel to *c*. As the axial 4*a* site becomes less nitride rich, the Ta—X bond distance increases by 0.22%, while as the equatorial 8*h* site becomes more nitride rich, the Ta—X bond distance decreases by 0.33%. The decrease in the mean Ta—X bond distance as the anions disorder is 0.15%. The mean distance in the anion-disordered form is 2.017 76(6) Å, similar to the distance expected on the basis of ionic radii.<sup>12</sup> However, the Ta—X bonding in this material is far from ionic: the *increase* in the axial distance as the proportion of nitride on the 4*a* site decreases is opposite to expectation based on the N<sup>3-</sup>

(11) Larson, A.; von Dreele, R. B. *The General Structure Analysis System*; Los Alamos National Laboratory: Los Alamos, NM, 1985.

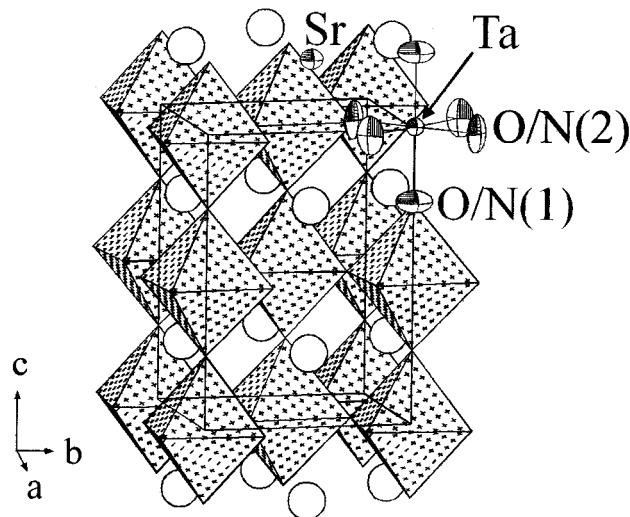


**Figure 2.** Structure of  $\text{SrTaO}_2\text{N}$ . Thermal ellipsoids are shown at the 99.9% confidence level.

ion having a larger radius (1.50 Å) than the  $\text{O}^{2-}$  ion (1.40 Å).<sup>13</sup> The shorter Ta–N distances are presumably a result of better orbital overlap and stronger covalent bonding than that between tantalum and oxygen.

**Structures of  $\text{A}_2\text{TaO}_3\text{N}$  ( $\text{A} = \text{Sr, Ba}$ ).** The model of Diot *et al.*<sup>14</sup> for  $\text{Sr}_2\text{TaO}_3\text{N}$  with the  $\text{K}_2\text{NiF}_4$  structure was used as the starting point for both phases. The refinement of their model in  $I\bar{4}/mm$  against data for our sample of  $\text{Sr}_2\text{TaO}_3\text{N}$  (Figure 3) showed that the materials prepared by the two routes are isostructural and have almost fully ordered anions with respect to the space group symmetry: one 4-fold site is occupied solely by oxide, and the other site contains all the nitride ions. Our higher synthesis temperature of 1500 °C does not promote O/N disorder in this case. Refinement of the oxide and nitride occupancies, with no restriction on stoichiometry but with both anion sites constrained to be fully occupied, produced the stoichiometry  $\text{Sr}_2\text{TaO}_{3.12(5)}\text{N}_{0.88(5)}$ , fairly consistent with the stoichiometry  $\text{Sr}_2\text{TaO}_{2.86(5)}\text{N}_{1.09(5)}$  obtained by TGA. A detailed structural investigation of  $\text{Ba}_2\text{TaO}_3\text{N}$  has previously been hampered by its extreme moisture sensitivity. Our refinement of a structural model for  $\text{Ba}_2\text{TaO}_3\text{N}$  based on that of  $\text{Sr}_2\text{TaO}_3\text{N}$  confirmed that the two materials are isostructural. The composition refined to  $\text{Ba}_2\text{TaO}_{3.03(2)}\text{N}_{0.97(2)}$ , in agreement with the stoichiometry of  $\text{Ba}_2\text{TaO}_{3.15(5)}\text{N}_{0.90(5)}$  derived from combustion analysis for nitrogen (reliable thermogravimetric analysis was not possible using our apparatus on account of the air sensitivity of the compound). 3.5% by mass of  $\text{BaTaO}_2\text{N}$  perovskite, not apparent in the PXRD pattern, was included in the refinement as a second phase. The refinement results for  $\text{Ba}_2\text{TaO}_3\text{N}$  are presented in Table 2, and the fit is shown in Figure 3. The two structures are compared in Tables 5 and 6.

### Discussion

Both the anion ordered<sup>3</sup> and anion disordered forms of the perovskite  $\text{SrTaO}_2\text{N}$  crystallize in the  $a^0a^0c^-$

(12) Lide, D. R., Ed. *CRC Handbook of Chemistry and Physics*, 81st ed.; CRC Press: Boca Raton, FL, 2000. Shannon, R. D. *Acta Crystallogr.* **1976**, *A32*, 751.

(13) Baur, W. H. *Crystallogr. Rev.* **1987**, *1*, 59.

(14) Diot, N.; Marchand, R.; Haines, J.; Leger, J. M.; Macaudiere, P.; Hull, S. *J. Solid State Chem.* **1999**, *146*, 390.

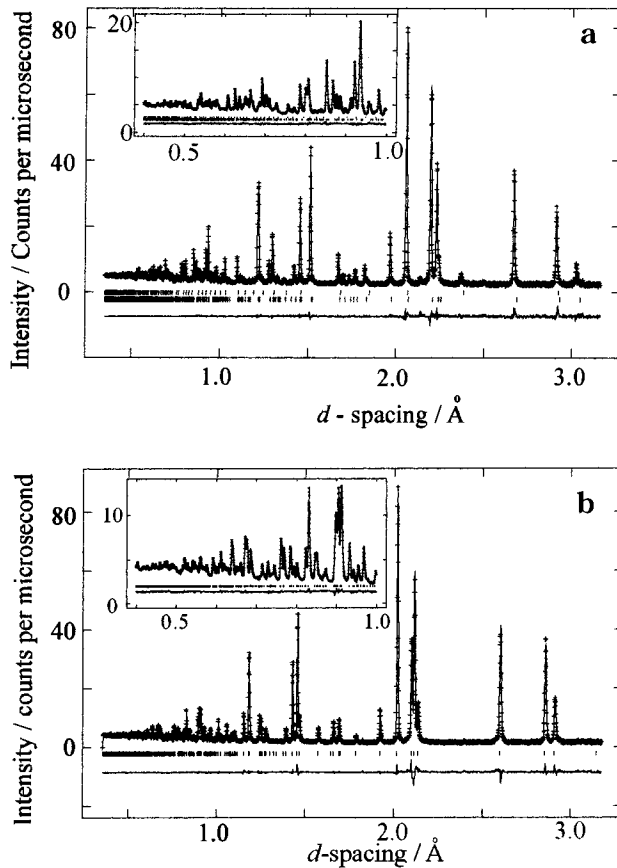


**Figure 3.** (a) Results of the refinement of the structure of  $\text{Ba}_2\text{TaO}_3\text{N}$  against powder neutron diffraction data (145° detector bank). The measured (points), calculated (line), and difference (lower line) profiles are shown. The sets of tick marks indicate allowed reflections for  $\text{Ba}_2\text{TaO}_3\text{N}$  (lower set) and the  $\text{BaTaO}_2\text{N}$  impurity (3.5% by mass; upper set). (b) Results of refinement of the structure of  $\text{Sr}_2\text{TaO}_3\text{N}$ .

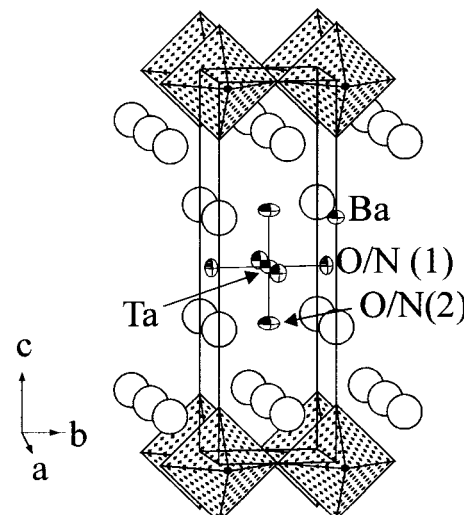


**Figure 4.** Structure of  $\text{Ba}_2\text{TaO}_3\text{N}$ . Thermal ellipsoids are shown at the 99.9% confidence level.

distorted perovskite structure according to the classification of Glazer.<sup>15</sup> The material synthesized by mineralizer-assisted nitridation of an oxide precursor using ammonia<sup>3</sup> displays full O/N order while the material described here, synthesized by conproportion-

(15) Glazer, A. M. *Acta Crystallogr.* **1972**, *B28*, 3384.

**Table 5. Atomic Positions for  $\text{Sr}_2\text{TaO}_3\text{N}$  and  $\text{Ba}_2\text{TaO}_3\text{N}$  Prepared at 1500 °C**

compound	atom	site	x	y	z	$100 U_{\text{iso},\text{eq}}^2/\text{\AA}^2$	oxide occupancy
$\text{Sr}_2\text{TaO}_3\text{N}$	Sr	4e	0	0	0.35409(3)	0.81(4)	
	Ta	2a	0	0	0	0.50(1)	
	O/N(1)	4c	0	0.5	0	0.95(2)	0.576(2) [0.57(1)] <sup>b</sup>
	O/N(2)	4e	0	0	0.16001(3)	1.50(7)	0.986(2) [0.93(1)] <sup>b</sup>
$\text{Ba}_2\text{TaO}_3\text{N}$	Ba	4e	0	0	0.35378(4)	0.68(4)	
	Ta	2a	0	0	0	0.71(1)	
	O/N(1)	4c	0	0.5	0	0.70(1)	0.545(4)
	O/N(2)	4e	0	0	0.15092(4)	0.98(2)	0.971(4)

<sup>a</sup> Equivalent isotropic displacement parameters are given; the anisotropic displacement ellipsoids for  $\text{Ba}_2\text{TaO}_3\text{N}$  are shown in Figure 4. <sup>b</sup> Values in square brackets refer to ref 14.

**Table 6. Interatomic Distances (Å) Determined for  $\text{Sr}_2\text{TaO}_3\text{N}$  and  $\text{Ba}_2\text{TaO}_3\text{N}^a$** 

bond	$\text{Sr}_2\text{TaO}_3\text{N}$		distance/Å for $\text{Ba}_2\text{TaO}_3\text{N}$
	this work	ref 14	
Ta—O/N(1) [4] <sup>b</sup>	2.01950(2)	2.021(1)	2.05754(1)
Ta—O/N(2) [2] <sup>b</sup>	2.0163(4)	2.020(1)	2.0190(5)
A—O/N(1) [4] <sup>b</sup>	2.7311(2)	2.728(1)	2.8390(4)
A—O/N(2) [4] <sup>b</sup>	2.86152(4)	2.864(1)	2.9105(1)
A—O/N(2) [1] <sup>b</sup>	2.4454(5)	2.451(1)	2.7138(5)

<sup>a</sup> All O/N—Ta—O/N angles are 90° or 180°. <sup>b</sup> Numbers in square brackets indicate the number of bonds of a particular type.

ation of binaries at a much higher temperature, reproduces the almost complete disorder observed by Marchand and co-workers<sup>4</sup> in material synthesized by ammonolysis of pure  $\text{Sr}_2\text{Ta}_2\text{O}_7$  (i.e. without the aid of a mineralizer). The observations of Jansen and co-workers<sup>3</sup> that a mineralizer promotes O/N order at 900 °C is consistent with that state being thermodynamically favored at that temperature and under the particular synthetic conditions employed. Our high-temperature reactions indicate that the O/N disordered state is favored, presumably on entropic grounds at 1500 °C. Full O/N order in oxynitrides is known for  $\text{TaON}^{16}$  with the baddeleyite structure and for the  $\text{K}_2\text{NiF}_4$ -structure oxynitrides  $\text{Nd}_2\text{AlO}_3\text{N}^1$  and  $\text{A}_2\text{TaO}_3\text{N}$  ( $\text{A} = \text{Sr, Ba}$ ) reported here (the O/N ordering scheme in the recently reported Ruddlesden–Popper strontium niobium oxynitrides<sup>17</sup> is as yet unexplored). In the case of perovskite oxynitrides, ordering is only observed (for  $\text{LaTaON}_2$  and  $\text{SrTaO}_2\text{N}^3$ ) when synthesis is mineralizer assisted. Generally, O/N disorder is observed in oxynitrides with the fairly isotropic cubic perovskite structure. In  $\text{BaTaO}_2\text{N}^{18}$ , which has the ideal cubic perovskite structure in  $Pm\bar{3}m$ , the lack of superstructure reflections in the neutron powder diffraction pattern precludes O/N order.

$\text{Ba}_2\text{TaO}_3\text{N}$ , like its previously described Sr counterpart,<sup>14</sup> has an anionic sublattice which is fully ordered with respect to the  $I4/mmm$  space group symmetry for the  $\text{K}_2\text{NiF}_4$  type cell, and in which exclusively the more electronegative oxide ion occupies the anion sites in the rock-salt layers, with the consequence that all the nitride ions statistically occupy the  $\text{Ta}(\text{O,N})_2$  planes in the perovskite layers. The ordering in these compounds contrasts strongly with that in  $\text{Nd}_2\text{AlO}_3\text{N}$ ,<sup>1</sup> which has the  $\text{K}_2\text{NiF}_4$  type structure with full O/N order but with nitride located exclusively on one of the axial sites of

the  $\text{AlO}_5\text{N}$  octahedron, and the space group symmetry lowered to  $I4mm$ . The ordering in  $\text{A}_2\text{TaO}_3\text{N}$  is consistent with the more polarizable nitride ions occupying exclusively  $\text{NTa}_2\text{A}_4$  octahedra while the anion site surrounded by a larger proportion of the less polarizing alkaline earth cation is populated solely by oxide to form  $\text{OTaA}_5$  octahedra. In  $\text{Nd}_2\text{AlO}_3\text{N}$ , the relative oxophilicities and polarizing abilities of  $\text{Nd}^{3+}$  and  $\text{Al}^{3+}$  differ less than those of  $\text{A}^{2+}$  and  $\text{Ta}^{5+}$  in the compounds considered here; hence, in  $\text{Nd}_2\text{AlO}_3\text{N}$ , nitride is in an octahedral  $\text{NAlNd}_5$  environment and oxide occupies  $\text{OAlNd}_5$  and  $\text{OAl}_2\text{Nd}_4$  environments. The  $\text{TaO}_4\text{N}_2$  octahedra in  $\text{A}_2\text{TaO}_3\text{N}$  ( $\text{A} = \text{Sr, Ba}$ ) are slightly compressed along the *c* axis: the axial Ta—O distances (Table 6) are 2.0163(4) Å and 2.0190(5) Å for  $\text{Sr}_2\text{TaO}_3\text{N}$  and  $\text{Ba}_2\text{TaO}_3\text{N}$ , respectively, while the equatorial Ta—(O,N) distances are 2.01950(1) and 2.05754(1) Å, respectively. This contrasts with the large elongation observed in  $\text{Nd}_2\text{AlO}_3\text{N}^1$  (axial Al—N and Al—O distances of 2.130(6) Å and 2.086(8) Å, respectively, and four equatorial Al—O distances of 1.855(1) Å), which accounts for the relatively large *c/a* ratio for  $\text{Nd}_2\text{AlO}_3\text{N}^1$  of 3.319 compared with values of *c/a* of 3.120 for  $\text{Sr}_2\text{TaO}_3\text{N}$  and of 3.251 for  $\text{Ba}_2\text{TaO}_3\text{N}$ . The regularity of the  $\text{TaO}_4\text{N}_2$  octahedra in  $\text{Sr}_2\text{TaO}_3\text{N}$  and  $\text{Ba}_2\text{TaO}_3\text{N}$  indicates that tantalum competes well against the alkaline earth cation for the anion. The mean Ta—(O,N) distances in  $\text{SrTaO}_2\text{N}$  (2.01776(6) Å) and  $\text{Sr}_2\text{TaO}_3\text{N}$  (2.0184(2) Å) are equal within three standard deviations. The mean distance in  $\text{Ba}_2\text{TaO}_3\text{N}$  is slightly longer: 2.0451(3) Å, to accommodate the larger  $\text{Ba}^{2+}$  cation. The effect of the larger  $\text{Ba}^{2+}$  cation is to slightly compress the  $\text{TaO}_4\text{N}_2$  octahedron relative to that in  $\text{Sr}_2\text{TaO}_3\text{N}$  and to increase the *c/a* ratio by 4.2%, from 3.120 in  $\text{Sr}_2\text{TaO}_3\text{N}$  to 3.251 in  $\text{Ba}_2\text{TaO}_3\text{N}$ .

## Conclusion

We have demonstrated the potential of using the high-temperature conproportionation route as a complement to nitridation by ammonolysis to make transition metal oxynitrides. The use of inductive heating allows the sample to be contained under a pure nitrogen atmosphere even at temperatures of 1500 °C or greater and thus allows the oxide content to be determined by the choice of starting composition. This should extend the range of accessible oxynitride phases, since in the traditional route of oxide ammonolysis the nitride content in the products is limited by the oxophilicity of the metals concerned. The highest oxidation state of electropositive early transition metals such as tantalum is maintained in nitride-containing ternary materials

(16) Armytage, D.; Fender, B. E. F. *Acta Crystallogr.* **1974**, *B30*, 809.

(17) Tobias, G.; Oró-Solé, J.; Beltrán-Porter, D.; Fuertes, A. *Inorg. Chem.* **2001**, *40*, 6867.

(18) Pors, F.; Marchand, R.; Laurent, Y.; Bacher, P.; Roult, G. *Mater. Res. Bull.* **1988**, *23*, 1447.

even at 1500 °C, providing that another electropositive metal is present in the ternary phase and that an atmosphere of N<sub>2</sub> is maintained over the sample. Oxide/nitride ordering is apparently thermodynamically disfavored in oxynitrides with isotropic structures, such as the cubic perovskite structure, especially when prepared at very high temperatures, although O/N ordered polymorphs may be obtained by the appropriate synthetic route.<sup>3</sup> Such O/N ordering is common in lower dimensional structures in which competition for the oxide and

nitride anions by the chemically different cations dictates the ordering scheme.

**Acknowledgment.** S.J.C. and M.J.R. thank the Engineering and Physical Sciences Research Council (EPSRC) for financial support, including the award of a studentship to C.W.M., and for access to ISIS. S.J.C. thanks the University of Oxford, The Royal Society, and the Nuffield Foundation for funding.

CM011738Y